

Deeper but smaller: Higher-order interactions increase linear stability but shrink basins

Yuanzhao Zhang,^{1,*} Per Sebastian Skardal,² Federico Battiston,³ Giovanni Petri,^{4,5,6} and Maxime Lucas^{5,†}

¹*Santa Fe Institute, Santa Fe, NM, USA*

²*Department of Mathematics, Trinity College, Hartford, CT 06106, USA*

³*Department of Network and Data Science, Central European University, 1100 Vienna, Austria*

⁴*NP Lab, Network Science Institute, Northeastern University London, London, UK*

⁵*CENTAI Institute, 10138 Torino, Italy*

⁶*IMT Lucca, Lucca, Italy*

A key challenge of nonlinear dynamics and network science is to understand how higher-order interactions influence collective dynamics. Although many studies have approached this question through linear stability analysis, less is known about how higher-order interactions shape the global organization of different states. Here, we shed light on this issue by analyzing the rich patterns supported by identical Kuramoto oscillators on hypergraphs. We show that higher-order interactions can have opposite effects on linear stability and basin stability: they stabilize twisted states (including full synchrony) by improving their linear stability, but also make them hard to find by dramatically reducing their basin size. Our results highlight the importance of understanding higher-order interactions from both local and global perspectives.

Higher-order interactions [1–5] connecting more than two units simultaneously are key in shaping complex dynamical processes such as contagion and evolution in social networks [6–10], information processing in the brain [11–14], and synchronization in coupled oscillators [15–17]. Understanding how they influence collective dynamics is thus essential. A variety of studies have approached this challenge from a linear stability perspective, which characterizes how states such as synchronization and consensus respond to small perturbations [18–29]. However, little attention has been paid to basin stability [30], a global measure based on the size of basins of attraction, which dictates the system’s response to large perturbations [31–35].

In this Letter, we provide a more complete picture of how higher-order interactions influence dynamical patterns, in terms of both linear and basin stability. We show that higher-order interactions can have opposite effects: they can create more sync states by making them linearly stable; at the same time, higher-order interactions also dramatically shrink their attraction basins, effectively hiding them. As a result, states such as full synchrony may be stable but unreachable from random initial conditions.

To demonstrate this point, we consider a popular model system— n identical phase oscillators coupled through both pairwise and triadic interactions:

$$\begin{aligned} \dot{\theta}_i = \omega &+ \frac{\sigma}{k_i^{(1)}} \sum_{j=1}^n A_{ij} \sin(\theta_j - \theta_i) \\ &+ \frac{\sigma_{\Delta}}{2k_i^{(2)}} \sum_{j,k=1}^n B_{ijk} \sin(\theta_j + \theta_k - 2\theta_i). \end{aligned} \quad (1)$$

Equation (1) is a natural generalization of the Kuramoto model [36], where $\theta_i \in S^1$ represents the phase of oscillator i and ω is their common frequency. The adjacency

tensors determine which oscillators interact: $A_{ij} = 1$ if nodes i and j have a pairwise connection, and zero otherwise. Similarly, $B_{ijk} = 1$ if and only if nodes i , j , and k are coupled through a triadic interaction. The coupling strengths are given by σ and σ_{Δ} , respectively, and are normalized by $k_i^{(\ell)}$, the ℓ th order degree of node i .

The case of pairwise coupling ($\sigma_{\Delta} = 0$) has been studied in detail from both linear and basin stability perspectives. While full synchrony $\theta_i(t) = \theta_j(t) \forall i, j, t$ is always an attractor of Eq. (1), additional attractors can emerge but only when networks are not too dense [37–40]. For ring networks, these attractors are *twisted states* and they emerge for link density below 0.68 [41]. In a q -twisted state $\theta^{(q)}$, the phases make q full twists around the ring and satisfy $\theta_k^{(q)} = 2\pi kq/n + C$, where q is the *winding number* [c.f. Fig. 1(a)]. In particular, the fully synchronized state corresponds to $q = 0$. For rings with nearest-neighbor couplings, the number of attractors grows linearly with n , since twisted states with up to $n/4$ twists are stable [42, 43]. A fruitful line of research aims to characterize the basins of the coexisting twisted states, which has revealed interesting scaling relations between basin size and winding number [41, 44, 45] as well as tentacle-like structures in the basins [45–47].

Here, we focus on an analytically tractable case of Eq. (1) equipped with a simple ring structure:

$$\begin{aligned} \dot{\theta}_i = \frac{\sigma}{2r} \sum_{j=i-r}^{i+r} \sin(\theta_j - \theta_i) \\ + \frac{\sigma_{\Delta}}{2r(2r-1)} \sum_{j=i-r}^{i+r} \sum_{k=i-r}^{i+r} \sin(\theta_j + \theta_k - 2\theta_i), \end{aligned} \quad (2)$$

where r is the coupling range. For the triadic coupling, we require $i \neq j \neq k$, so that each triangle involves three distinct nodes. Notice that we have set $\omega = 0$ by going

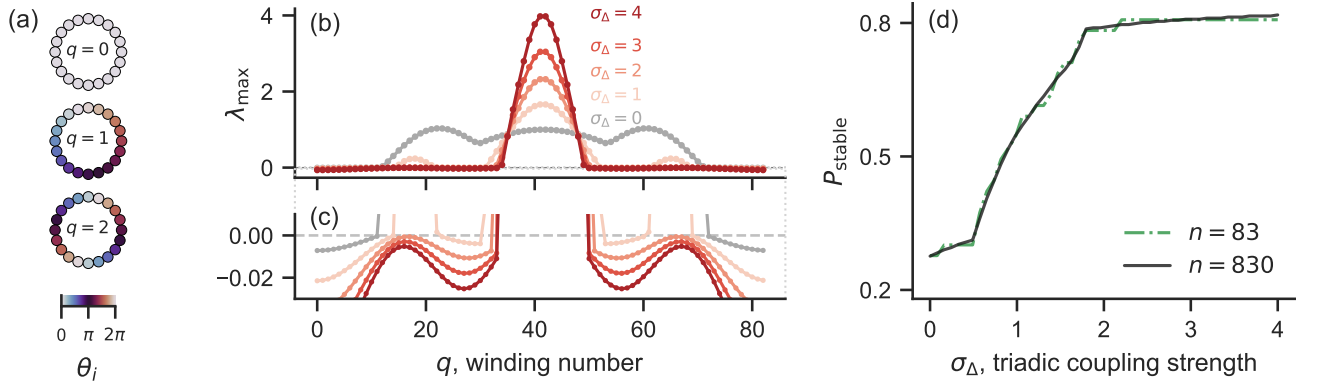


FIG. 1. **Higher-order interactions improve the linear stability of twisted states.** (a) Example twisted states with different winding numbers, for $n = 20$. Full synchrony corresponds to $q = 0$. (b) Linear stability (measured by the largest transverse Lyapunov exponent λ_{\max}) of q -twisted states, for a range of triadic coupling strengths σ_{Δ} . (c) Zoom-in view around $\lambda_{\max} = 0$ showing which twisted states are stable ($\lambda_{\max} < 0$). More twisted states become stable as σ_{Δ} is increased. (d) Fraction of twisted states that are stable as a function of σ_{Δ} , for $n = 83$ and $n = 830$.

into a rotating frame. Also note that we can always set $\sigma = 1$ by rescaling time, which we adopt throughout the rest of the Letter. For demonstration purposes, all numerical results below are presented for Eq. (2) with $n = 83$ and $r = 2$, unless otherwise stated. The key findings remain qualitatively unchanged for other choices of the parameters [48].

Due to the rotational symmetry, twisted states are solutions to Eq. (2). We first show that triadic interactions can stabilize twisted states far beyond what is possible with pairwise coupling. To analyze the linear stability of any fixed-point solution θ^* of Eq. (1), we can write down the Jacobian $\mathbf{J}(\theta^*) = \mathbf{J}^{(1)}(\theta^*) + \mathbf{J}^{(2)}(\theta^*)$, where

$$\begin{aligned} J_{ij}^{(1)}(\theta^*) &= \frac{\sigma}{k_i^{(1)}} A_{ij} \cos(\theta_j^* - \theta_i^*), \\ J_{ij}^{(2)}(\theta^*) &= \frac{\sigma_{\Delta}}{k_i^{(2)}} \sum_{k=1}^n B_{ijk} \cos(\theta_j^* + \theta_k^* - 2\theta_i^*) \end{aligned} \quad (3)$$

for $i \neq j$ and $J_{ii}^{(\ell)} = -\sum_{j=1}^n J_{ij}^{(\ell)}$. For the rotationally symmetric topology considered in Eq. (2), the Jacobian is a symmetric circulant matrix of the form

$$\mathbf{J} = \begin{bmatrix} J_0 & J_1 & J_2 & \cdots & J_2 & J_1 \\ J_1 & J_0 & J_1 & \cdots & J_3 & J_2 \\ \vdots & \vdots & \vdots & \ddots & \vdots & \vdots \\ J_1 & J_2 & J_3 & \cdots & J_1 & J_0 \end{bmatrix}. \quad (4)$$

We know that the normalized eigenvectors of a circulant matrix are the Fourier modes and the eigenvalues of \mathbf{J} are given by

$$\lambda_p(\mathbf{J}) = \sum_{s=0}^{n-1} J_s e^{2\pi i p s / n}, \quad 0 \leq p \leq n-1, \quad (5)$$

where $J_s = J_{n-s}$ for $\lfloor n/2 \rfloor < s < n$ [49]. This implies that λ_p are all real. Moreover, λ_0 is always equal to 0,

and it represents the mode for which all oscillators are perturbed by the same amount. For any q -twisted state, $\theta^{(q)}$, J_s is given by

$$\begin{aligned} J_s &= \frac{\sigma}{2r} \cos\left(\frac{2\pi q}{n} s\right) + \frac{\sigma_{\Delta}}{r(2r-1)} \sum_{k=-r}^r \cos\left(\frac{2\pi q}{n}(s+k)\right) \\ &\quad - \frac{\sigma_{\Delta}}{r(2r-1)} \sum_{j=1}^2 \cos\left(\frac{2\pi q}{n} j s\right) \text{ for } 0 < s \leq r, \\ J_s &= 0 \text{ for } s > r, \\ J_0 &= -2 \sum_{s=1}^r J_s. \end{aligned}$$

For example, for $r = 2$,

$$\begin{aligned} J_1 &= \frac{\sigma}{4} \cos\left(\frac{2\pi q}{n}\right) + \frac{\sigma_{\Delta}}{6} \left[1 + \cos\left(\frac{2\pi q}{n}\right) + \cos\left(\frac{6\pi q}{n}\right) \right], \\ J_2 &= \frac{\sigma}{4} \cos\left(\frac{4\pi q}{n}\right) + \frac{\sigma_{\Delta}}{6} \left[1 + \cos\left(\frac{2\pi q}{n}\right) + \cos\left(\frac{6\pi q}{n}\right) \right]. \end{aligned}$$

Plugging the formula for J_s into Eq. (5), we can analytically obtain the spectrum of the Jacobian for any q -twisted state and any coupling range r .

In Fig. 1(b)-(c), we show the linear stability of twisted states, measured by $\lambda_{\max} = \max\{\lambda_1, \lambda_2, \dots, \lambda_{n-1}\}$, as a function of the winding number q . We first note that the plot is symmetric with respect to $q = \frac{n}{2}$. This follows from the fact that twisted states with winding numbers q and $n-q$ are the same up to the reversal symmetry $\theta \rightarrow -\theta$ (the same symmetry applies to q and $-q$). Thus, below we will only consider $0 \leq q \leq \lfloor \frac{n}{2} \rfloor$. At $\sigma_{\Delta} = 0$, the stability curve has three peaks, and λ_{\max} becomes positive for $q > 11$. Thus, pairwise coupling in Eq. (2) cannot support stable twisted states with more than 11 twists (for $n = 83$ and $r = 2$). For systems with strong triadic couplings, the two side peaks are flattened while

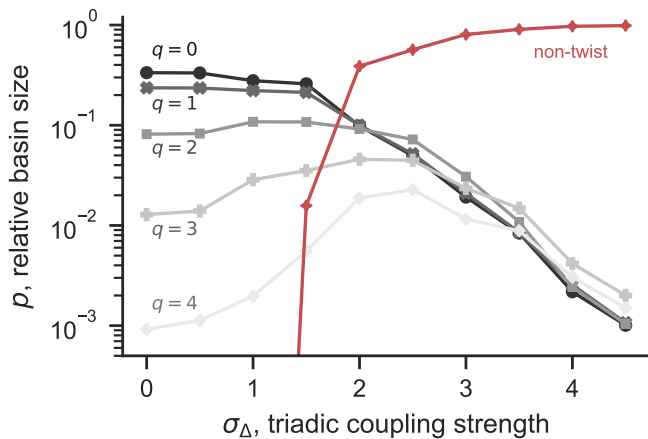


FIG. 2. **Higher-order interactions decrease the basin stability of twisted states.** We show p , the relative basin size, as a function of the triadic coupling strength σ_Δ . We estimated p by simulations starting from 10^5 random initial conditions. Each line represents a q -twisted state, except the red line, which represents attractors that are not twisted states. The relative basin size of non-twisted states quickly approaches 1 as σ_Δ is increased. We only show $q \geq 0$ due to the symmetry between q and $-q$.

the central peak becomes more prominent. As a result, a lot more twisted states become stable. For example, all twisted states up to 33 twists are stable for $\sigma_\Delta = 4$. Interestingly, for intermediate σ_Δ , because λ_{\max} is a nonmonotonic function of q , winding numbers on disjoint intervals can become stabilized. For instance, at $\sigma_\Delta = 1$, twisted states are stable for $q \leq 14$, become unstable for $14 < q < 23$, then become stable again for $23 \leq q \leq 30$ (see Fig. 1(c) for details).

Figure 1(d) shows the fraction of stable twisted states P_{stable} as a function of σ_Δ , which further emphasizes the dramatic number of twisted states stabilized by triadic interactions. We see that P_{stable} is monotonically increasing with σ_Δ , and that one can easily go from less than 30% of stable twisted states to over 80% stable by adding triadic interactions. We also show the same curve for a larger system with $n = 830$, which is basically a smoother version of $n = 83$ (since there are a lot more twisted states for $n = 830$). Our results echo the recent findings in Ref. [50], which showed that higher-order interactions can stabilize twisted states in graphons.

Next, we switch to the basin stability perspective. Figure 2 shows how the relative basin size p of the twisted states change with the triadic coupling strength σ_Δ . For $\sigma_\Delta = 0$, twisted states (including full synchrony), are the only stable states and thus take up the entire state space. States with fewer twists (smaller q) have a larger basin size. In particular, full synchrony attracts the most initial conditions. Now, for small σ_Δ , triadic interactions are affecting twisted states unequally: the basins for small q shrink whereas those for large q expand. As σ_Δ is fur-

ther increased, the basins for the non-twisted states appear and quickly become dominant, whereas the basins of the twisted states all shrink and become comparable in size. Note that, among the twisted states, full synchrony does not have the largest basin anymore—in fact, the twisted state with the largest basin has more twists as σ_Δ is increased.

Figure 3 further illustrates the opposite effects of higher-order interactions on linear stability and basin stability by visualizing the morphology of basins as σ_Δ is increased. Specifically, we examine a random 2D slice of the state space, spanned by $\theta_0 + \alpha_1 \mathbf{P}_1 + \alpha_2 \mathbf{P}_2$, $\alpha_i \in (-\pi, \pi]$. Here, \mathbf{P}_1 and \mathbf{P}_2 are n -dimensional binary orientation vectors in which $\lfloor n/2 \rfloor$ randomly selected components are 1 and the rest of the components are 0. We set the origin to be the twisted state with $q = 12$, $\theta_0 = \theta^{(12)}$, which we know from Fig. 1 is unstable when $\sigma_\Delta = 0$. Thus, we can only see basins for q between -3 and 7 in Fig. 3(a). Adding triadic interactions stabilizes $q = 12$, so we see its basin emerge in Fig. 3(b) when σ_Δ is set to 1. For larger σ_Δ shown in panels (c) and (d), the reduction in basin stability for twisted states becomes apparent. Despite their significantly improved linear stability, the basins for twisted states (as a group) rapidly shrink as more and more points get absorbed into the basin for non-twisted states (colored black), making twisted states hard to reach from random initial conditions.

The natural next question is: What are those non-twisted states created by higher-order interactions? Figure 4 shows that they consist of chimera states with increasingly large disordered domains as triadic couplings become stronger. Here, P_{order} measures the portion of oscillators that are ordered. Twisted states correspond to $P_{\text{order}} = 1$ and disordered states correspond to $P_{\text{order}} \approx 0$, whereas chimera states have P_{order} between 0 and 1. For final states reached from random initial conditions, the average P_{order} decreases from 1 to 0 as σ_Δ is increased.

We classify oscillators as (dis)ordered by calculating the local order parameters

$$O_j = \frac{1}{2r+1} \sum_{k=j-r}^{j+r} e^{i\theta_k}, \quad (6)$$

for $j = 1, \dots, n$. We classify oscillator j as disordered if $|O_j| < 0.85$ [51]. The insets show typical attractors for different values of σ_Δ . Despite the fact that more and more twisted states become linearly stable for larger σ_Δ , they are increasingly unlikely to be observed from random initial conditions. Instead, the state space is dominated by the basins for chimera states (intermediate σ_Δ) or disordered states (large σ_Δ). This is consistent with recent results showing that higher-order interactions promote chimera states in simplicial complexes [52]. We note that here the disorder is only in space, not in time—the patterns remain frozen over time and all oscillators are phase-locked [53].

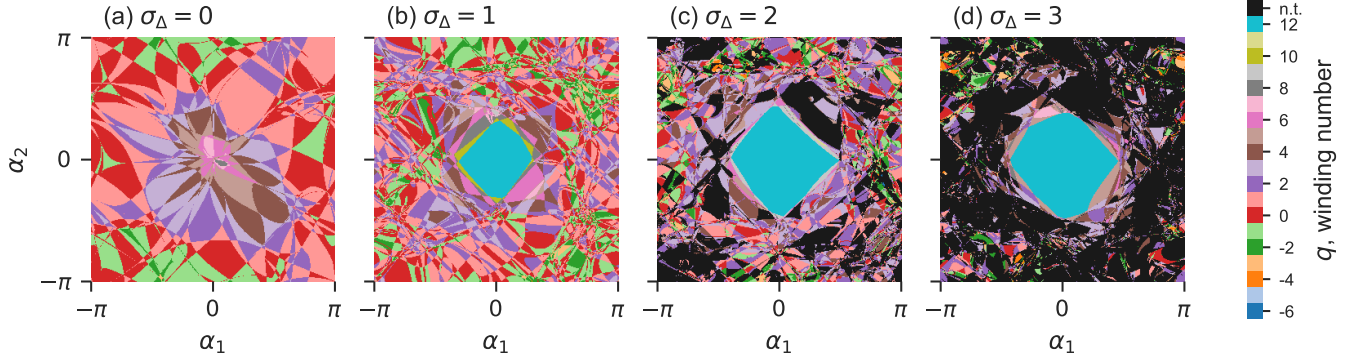


FIG. 3. **Higher-order interactions stabilize twisted states but shrink their basins.** Two-dimensional slices of the state space (centered around the twisted state with $q = 12$) showing how basins change as σ_Δ is increased. The basins of the twisted states are colored according to their winding number q , and the basins of all other states are colored black. (a) For $\sigma_\Delta = 0$, the twisted state with $q = 12$ is unstable, and all points converge to a twisted state with a lower winding number. (b) For $\sigma_\Delta = 1$, all attractors are still twisted states. Moreover, $q = 12$ becomes stable, which creates the cyan basin at the center. (c, d) For stronger triadic interactions ($\sigma_\Delta = 2$ and 3), the $q = 12$ basin expands, but non-twisted states also start to appear and quickly become dominant. Although the basin for $q = 12$ looks significant on the 2D slices, due to the high-dimensional nature of the state space, it would be almost impossible to reach from random initial conditions.

Aside from the generalization of Kuramoto models introduced in Eq. (2), there are several other natural ways to introduce triadic interactions that would preserve twisted states. For example, we can turn the ring network into a simplicial (flag) complex by filling all pairwise triangles. This implies that $B_{ijk} = 1$ if and only if $i \neq j \neq k$, and all three pairs are within distance r : $|(i - j) \bmod n| \leq r$, $|(i - k) \bmod n| \leq r$, and $|(j - k) \bmod n| \leq r$. In other words, $B_{ijk} = A_{ij}A_{ik}A_{jk}$. In comparison, the topologies considered in Eq. (2) do not require $|(j - k) \bmod n| \leq r$ for $B_{ijk} = 1$. This can be

expressed equivalently as $B_{ijk} = A_{ij}A_{ik}$. Although a systematic investigation of the effects of topology is beyond the scope of this Letter, we confirm that the main results presented here remain valid for (ring) simplicial complexes and for arbitrary coupling range r . We also tested the effects of higher-order interactions on random hypergraphs. There, the only twisted state that can be an attractor is full synchrony ($q = 0$). Similar to what we found here for more regular structures, in random hypergraphs triadic interactions make full sync more linearly stable [18, 27] but its basin of attraction shrinks dramatically in favor of more disordered states.

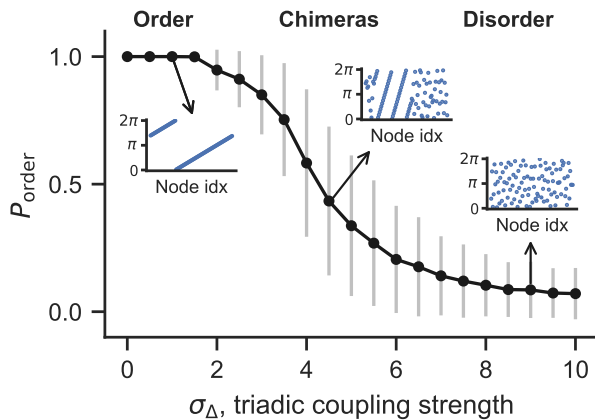


FIG. 4. **Chimeras bridge the transition from order to disorder as triadic interactions become stronger.** As we increase σ_Δ , we have a smooth transition from order (twisted states) to chimeras, and then to disorder. We monitor the transition by computing the portion of ordered oscillators P_{order} in the final state, averaged over 1000 simulations from random initial conditions for each σ_Δ . The error bars represent standard deviations and the insets show typical attractors reached from random initial conditions.

Why do the basins of twisted states shrink as higher-order couplings are introduced? Extensive multistability induced by higher-order interactions has been observed under many different settings [52, 54–57]. Such multistability is also at the core of the phenomenon of basin shrinking described here. This raises the question of its mechanism, condition, and generality. Does multistability emerge naturally from generic higher-order interactions regardless of details about the dynamics and couplings? A promising direction would be to investigate this question from the energy landscape perspective and characterize the relation between multi-body interactions and the ruggedness of the landscape. It would also be interesting to study Eq. (2) in the thermodynamic limit and look for a set of reduced equations in the spirit of Ott-Antonsen ansatz [58], which may provide further insights into the origin of chimera and disordered states. In conclusion, we hope this work will stimulate future endeavors to understand the effects of higher-order interactions from both local and global perspectives.

We thank Melvyn Tyloo for insightful discussions. Y.Z. acknowledges support from the Omidyar Fellowship.

* yzhang@santafe.edu

† maxime.lucas@centai.eu

- [1] F. Battiston, G. Cencetti, I. Iacopini, V. Latora, M. Lucas, A. Patania, J.-G. Young, and G. Petri, Networks beyond pairwise interactions: Structure and dynamics, *Phys. Rep.* **874**, 1 (2020).
- [2] L. Torres, A. S. Blevins, D. Bassett, and T. Eliassi-Rad, The why, how, and when of representations for complex systems, *SIAM Rev.* **63**, 435 (2021).
- [3] F. Battiston, E. Amico, A. Barrat, G. Bianconi, G. Ferraz de Arruda, B. Franceschiello, I. Iacopini, S. Kéfi, V. Latora, Y. Moreno, M. M. Murray, T. P. Peixoto, F. Vaccarino, and G. Petri, The physics of higher-order interactions in complex systems, *Nat. Phys.* **17**, 1093 (2021).
- [4] C. Bick, E. Gross, H. A. Harrington, and M. T. Schaub, What are higher-order networks?, *SIAM Rev.* **65**, 686 (2023).
- [5] F. Battiston and G. Petri, *Higher-Order Systems* (Springer, 2022).
- [6] I. Iacopini, G. Petri, A. Barrat, and V. Latora, Simplicial models of social contagion, *Nat. Commun.* **10**, 2485 (2019).
- [7] M. Lucas, I. Iacopini, T. Robiglio, A. Barrat, and G. Petri, Simplicially driven simple contagion, *Phys. Rev. Res.* **5**, 013201 (2023).
- [8] N. W. Landry and J. G. Restrepo, The effect of heterogeneity on hypergraph contagion models, *Chaos* **30**, 103117 (2020).
- [9] G. St-Onge, H. Sun, A. Allard, L. Hébert-Dufresne, and G. Bianconi, Universal nonlinear infection kernel from heterogeneous exposure on higher-order networks, *Phys. Rev. Lett.* **127**, 158301 (2021).
- [10] U. Alvarez-Rodriguez, F. Battiston, G. F. de Arruda, Y. Moreno, M. Perc, and V. Latora, Evolutionary dynamics of higher-order interactions in social networks, *Nat. Hum. Behav* **5**, 586 (2021).
- [11] G. Petri, P. Expert, F. Turkheimer, R. Carhart-Harris, D. Nutt, P. J. Hellyer, and F. Vaccarino, Homological scaffolds of brain functional networks, *J. R. Soc. Interface* **11**, 20140873 (2014).
- [12] C. Giusti, R. Ghrist, and D. S. Bassett, Two's company, three (or more) is a simplex: Algebraic-topological tools for understanding higher-order structure in neural data, *J Comput Neurosci.* **41**, 1 (2016).
- [13] F. Parastesh, M. Mehrabbeik, K. Rajagopal, S. Jafari, and M. Perc, Synchronization in Hindmarsh–Rose neurons subject to higher-order interactions, *Chaos* **32**, 013125 (2022).
- [14] A. Santoro, F. Battiston, G. Petri, and E. Amico, Higher-order organization of multivariate time series, *Nat. Phys.* **19**, 221 (2023).
- [15] I. León and D. Pazó, Phase reduction beyond the first order: The case of the mean-field complex Ginzburg-Landau equation, *Phys. Rev. E* **100**, 012211 (2019).
- [16] M. H. Matheny, J. Emenheiser, W. Fon, A. Chapman, A. Salova, M. Rohden, J. Li, M. Hudoba de Bady, M. Pósfai, L. Duenas-Osorio, *et al.*, Exotic states in a simple network of nanoelectromechanical oscillators, *Science* **363**, eaav7932 (2019).
- [17] E. Engel, E. Teichmann, M. Rosenblum, and A. Pikovsky, High-order phase reduction for coupled oscillators, *J. phys. Complex* **2**, 015005 (2020).
- [18] M. Lucas, G. Cencetti, and F. Battiston, Multiorder Laplacian for synchronization in higher-order networks, *Phys. Rev. Res.* **2**, 033410 (2020).
- [19] A. P. Millán, J. J. Torres, and G. Bianconi, Explosive Higher-Order Kuramoto Dynamics on Simplicial Complexes, *Phys. Rev. Lett.* **124**, 218301 (2020).
- [20] L. Neuhäuser, A. Mellor, and R. Lambiotte, Multibody interactions and nonlinear consensus dynamics on networked systems, *Phys. Rev. E* **101**, 032310 (2020).
- [21] P. S. Skardal, L. Arola-Fernández, D. Taylor, and A. Arenas, Higher-order interactions can better optimize network synchronization, *Phys. Rev. Res.* **3**, 043193 (2021).
- [22] Y. Zhang, V. Latora, and A. E. Motter, Unified treatment of synchronization patterns in generalized networks with higher-order, multilayer, and temporal interactions, *Commun. Phys.* **4**, 195 (2021).
- [23] A. Salova and R. M. D'Souza, Cluster synchronization on hypergraphs, arXiv:2101.05464 (2021).
- [24] G. Ferraz de Arruda, M. Tizzani, and Y. Moreno, Phase transitions and stability of dynamical processes on hypergraphs, *Commun. Phys.* **4**, 24 (2021).
- [25] L. V. Gambuzza, F. Di Patti, L. Gallo, S. Lepri, M. Romance, R. Criado, M. Frasca, V. Latora, and S. Boccaletti, Stability of synchronization in simplicial complexes, *Nat. Commun.* **12**, 1255 (2021).
- [26] L. Gallo, R. Muolo, L. V. Gambuzza, V. Latora, M. Frasca, and T. Carletti, Synchronization induced by directed higher-order interactions, *Commun. Phys.* **5**, 263 (2022).
- [27] Y. Zhang, M. Lucas, and F. Battiston, Higher-order interactions shape collective dynamics differently in hypergraphs and simplicial complexes, *Nat. Commun.* **14**, 1605 (2023).
- [28] T. Carletti, L. Giambagli, and G. Bianconi, Global Topological Synchronization on Simplicial and Cell Complexes, *Phys. Rev. Lett.* **130**, 187401 (2023).
- [29] M. Nurisso, A. Arnaudon, M. Lucas, R. L. Peach, P. Expert, F. Vaccarino, and G. Petri, A unified framework for Simplicial Kuramoto models, arXiv:2305.17977 (2023).
- [30] P. J. Menck, J. Heitzig, N. Marwan, and J. Kurths, How basin stability complements the linear-stability paradigm, *Nat. Phys.* **9**, 89 (2013).
- [31] J. Milnor, On the concept of attractor, *Commun. Math.* **99**, 177 (1985).
- [32] E. Ott, *Chaos in dynamical systems* (Cambridge university press, 2002).
- [33] J. Aguirre, R. L. Viana, and M. A. Sanjuán, Fractal structures in nonlinear dynamics, *Rev. Mod. Phys.* **81**, 333 (2009).
- [34] P. J. Menck, J. Heitzig, J. Kurths, and H. Joachim Schellnhuber, How dead ends undermine power grid stability, *Nat. Commun.* **5**, 3969 (2014).
- [35] Y. Zhang, Z. G. Nicolaou, J. D. Hart, R. Roy, and A. E. Motter, Critical switching in globally attractive chimeras, *Phys. Rev. X* **10**, 011044 (2020).
- [36] S. H. Strogatz, From Kuramoto to Crawford: Exploring the onset of synchronization in populations of coupled oscillators, *Physica D* **143**, 1 (2000).
- [37] A. Townsend, M. Stillman, and S. H. Strogatz, Dense networks that do not synchronize and sparse ones that do, *Chaos* **30**, 083142 (2020).
- [38] M. Kassabov, S. H. Strogatz, and A. Townsend, Suffi-

- ciently dense Kuramoto networks are globally synchronizing, *Chaos* **31**, 073135 (2021).
- [39] M. Kassabov, S. H. Strogatz, and A. Townsend, A global synchronization theorem for oscillators on a random graph, *Chaos* **32**, 093119 (2022).
- [40] P. Abdalla, A. S. Bandeira, M. Kassabov, V. Souza, S. H. Strogatz, and A. Townsend, Expander graphs are globally synchronising, arXiv:2210.12788 (2022).
- [41] D. A. Wiley, S. H. Strogatz, and M. Girvan, The size of the sync basin, *Chaos* **16**, 015103 (2006).
- [42] R. Delabays, T. Coletta, and P. Jacquod, Multistability of phase-locking and topological winding numbers in locally coupled Kuramoto models on single-loop networks, *J. Math. Phys.* **57**, 032701 (2016).
- [43] D. Manik, M. Timme, and D. Witthaut, Cycle flows and multistability in oscillatory networks, *Chaos* **27**, 083123 (2017).
- [44] R. Delabays, M. Tyloo, and P. Jacquod, The size of the sync basin revisited, *Chaos* **27**, 103109 (2017).
- [45] Y. Zhang and S. H. Strogatz, Basins with tentacles, *Phys. Rev. Lett.* **127**, 194101 (2021).
- [46] S. Ashwin, J. Blawdziewicz, C. S. O’Hern, and M. D. Shattuck, Calculations of the structure of basin volumes for mechanically stable packings, *Phys. Rev. E* **85**, 061307 (2012).
- [47] S. Martiniani, K. J. Schrenk, J. D. Stevenson, D. J. Wales, and D. Frenkel, Structural analysis of high-dimensional basins of attraction, *Phys. Rev. E* **94**, 031301 (2016).
- [48] Our code is available online at https://github.com/maximelucas/basins_and_triangles. It uses XGI [59] and SciPy integrators [60]. For each initial condition, we integrated system (2) over 600 time units with a standard Runge-Kutta 45 scheme adopting adaptive stepsizes.
- [49] P. J. Davis, *Circulant matrices*, Vol. 2 (Wiley New York, 1979).
- [50] C. Bick, T. Böhle, and C. Kuehn, Phase oscillator networks with nonlocal higher-order interactions: Twisted states, stability, and bifurcations, *SIAM J. Appl. Dyn. Syst.* **22**, 1590 (2023).
- [51] Other threshold values result in similar curves. The value of 0.85 is large enough to ensure $P_{\text{order}} \simeq 0$ for large σ_{Δ} , which matches visual inspection of the states.
- [52] S. Kundu and D. Ghosh, Higher-order interactions promote chimera states, *Phys. Rev. E* **105**, L042202 (2022).
- [53] This is in contrast to traditional chimeras, for which the disordered oscillators are not synchronized and their relative phases change over time.
- [54] T. Tanaka and T. Aoyagi, Multistable attractors in a network of phase oscillators with three-body interactions, *Phys. Rev. Lett.* **106**, 224101 (2011).
- [55] P. S. Skardal and A. Arenas, Abrupt desynchronization and extensive multistability in globally coupled oscillator simplexes, *Phys. Rev. Lett.* **122**, 248301 (2019).
- [56] P. S. Skardal and A. Arenas, Higher order interactions in complex networks of phase oscillators promote abrupt synchronization switching, *Commun. Phys.* **3**, 218 (2020).
- [57] P. S. Skardal, S. Adhikari, and J. G. Restrepo, Multistability in coupled oscillator systems with higher-order interactions and community structure, *Chaos* **33**, 023140 (2023).
- [58] E. Ott and T. M. Antonsen, Low dimensional behavior of large systems of globally coupled oscillators, *Chaos* **18**, 037113 (2008).
- [59] N. W. Landry, M. Lucas, I. Iacopini, G. Petri, A. Schwarze, A. Patania, and L. Torres, XGI: A Python package for higher-order interaction networks, *J. Open Source Softw.* **8**, 5162 (2023).
- [60] P. Virtanen, R. Gommers, T. E. Oliphant, M. Haberland, T. Reddy, D. Cournapeau, E. Burovski, P. Peterson, W. Weckesser, J. Bright, S. J. van der Walt, M. Brett, J. Wilson, K. J. Millman, N. Mayorov, A. R. J. Nelson, E. Jones, R. Kern, E. Larson, C. J. Carey, Í. Polat, Y. Feng, E. W. Moore, J. VanderPlas, D. Laxalde, J. Perktold, R. Cimrman, I. Henriksen, E. A. Quintero, C. R. Harris, A. M. Archibald, A. H. Ribeiro, F. Pedregosa, P. van Mulbregt, and SciPy 1.0 Contributors, SciPy 1.0: Fundamental Algorithms for Scientific Computing in Python, *Nat. Methods* **17**, 261 (2020).